Atmos. Chem. Phys. Discuss., 8, 4309–4351, 2008
www.atmos-chem-phys-discuss.net/8/4309/2008/


Atmospheric Chemistry and Physics Discussions

# Comparison of OMI ozone and UV irradiance data with ground-based measurements at two French sites

**V. Buchard[1], C. Brogniez[1], F. Auriol[1], B. Bonnel[1], J. Lenoble[1,2], A. Tanskanen[3], B. Bojkov[4,5], and P. Veefkind[6]**

[1]Laboratoire d'Optique Atmosphérique, Université des Sciences et Technologies de Lille, France
[2]Interaction Rayonnement Solaire Atmosphère, Université Joseph Fourier de Grenoble, France
[3]Finnish Meteorological Institute, Helsinki, Finland
[4]Goddard Earth Sciences and Technology Center, University of Maryland, Baltimore County, Baltimore, Maryland, USA
[5]Atmospheric Chemistry Dynamics Branch, NASA Goddard Space Flight Center, Greenbelt, Maryland, USA
[6]Royal Netherlands Meteorological Institute, De Bilt, The Netherlands

Received: 18 January 2008 – Accepted: 25 January 2008 – Published: 3 March 2008

Correspondence to: V. Buchard (buchard@loa.univ-lille1.fr)

Published by Copernicus Publications on behalf of the European Geosciences Union.





## Abstract

Ozone Monitoring Instrument (OMI), launched in July 2004, is dedicated to the monitoring of the Earth's ozone, air quality and climate. OMI provides among other things the total column of ozone (TOC), the surface ultraviolet (UV) irradiance at several wavelengths, the erythemal dose rate and the erythemal daily dose. The main objective of this work is to validate OMI data with ground-based instruments in order to use OMI products (collection 2) for scientific studies. The Laboratoire d'Optique Atmosphérique (LOA) located in Villeneuve d'Ascq in the north of France performs solar UV measurements using a spectroradiometer and a broadband radiometer. The site of Briançon in the French Southern Alps is also equipped with a spectroradiometer operated by Interaction Rayonnement Solaire Atmosphère (IRSA). The instrument belongs to the Centre Européen Médical et Bioclimatologique de Recherche et d'Enseignement Supérieur. The comparison between the TOC retrieved with ground-based measurements and OMI TOC shows good agreement at both sites for all sky conditions. Comparisons of spectral UV on clear sky conditions are also satisfying whereas results of comparisons of the erythemal daily doses and erythemal dose rates for all sky conditions and for clear sky show that OMI overestimates significantly surface UV doses at both sites.

## 1 Introduction

The solar UV radiation has a large impact on human life, animals and plants, with both positive and negative effects. For example, exposure to solar UV enables the synthesis of vitamin D in skin whereas skin cancer or eye diseases can be caused by excessive doses of UV radiation (WMO, 2007). Atmospheric ozone is one of the main factors affecting the surface UV radiation, so its decline observed at middle and high latitudes since the 80's has led to monitoring of atmospheric ozone content and UV radiation. Ground-based instruments devoted to this monitoring have been developed in many countries as well as satellite instruments which allow a global geographical coverage.



ACPD

8, 4309–4351, 2008



Satellite data are affected by instrumental errors, as data from ground-based instruments (Bernhard and Seckmeyer, 1999), but are also affected by modelling uncertainties in deriving surface UV irradiance from UV radiance measured at the top of atmosphere. Therefore satellite derived products need to be validated with ground-based measurements. The TOC inferred from satellite measurements requests also validation. All these validations must be achieved with care because of a scale issue, indeed ground-based measurements are representative only of a small local area whereas satellite measurements are representative of a large region (OMI pixel at nadir $\sim 13 \times 24\,km^2$) so that difficulties can arise from the cloud or aerosol variability.

The ground-based instruments used to perform spectral irradiance measurements and the OMI instrument are described in Sect. 2 along with the methodologies for inferring the TOC and surface UV from ground-based and from OMI measurements. Section 3 presents comparisons between the OMI products and the products retrieved at two French sites, Villeneuve d'Ascq (50.61° N, 3.14° E, 70 m a.s.l.) and Briançon (44.90° N, 6.65° E, 1330 m a.s.l.). Section 4 reports the conclusions.

## 2 Instruments and methodologies

### 2.1 Ground-based instruments

Measurements of the instruments located at Villeneuve d'Ascq (VdA) and Briançon are used in this study. These sites are typical respectively of a flat region in the north of France and a high altitude valley of the French Southern Alps.

The spectroradiometers at VdA and Briançon are thermally regulated Jobin Yvon H10 double monochromators, and they scan the wavelength range from 280 to 450 nm with a sampling step of 0.5 nm. Their spectral resolution is about 0.7 nm (FWHM). Calibration is performed every 3 months with two standard lamps traceable to NIST and NPL, leading to an irradiance expanded uncertainty (coverage factor $k$=2) of about 8% at 300 nm and about 5% at 400 nm for a high irradiance level and 10% and



ACPD
8, 4309–4351, 2008



7% respectively for a low irradiance level. The instrument has been checked within the QASUME project in September 2004 (Intercomparison with the travelling standard spectroradiometer B5503 from Physikalisch-Meteorologisches Observatorium Davos, World Radiation Center, Switzerland). The spectroradiometers perform scans of the global irradiance from sunrise to sunset every 30 min. A single spectral scan takes about 6 min.

The broadband instrument in VdA is a UVB-1 type from Yankee Environmental System (YES), it delivers measurements of erythemal dose rate with a three minutes time frequency. It was calibrated in August 2006 during COST campaign.

#### 2.1.1 Ozone retrieval

The total ozone column is routinely retrieved from the ground-based global irradiance spectrum using a differential absorption technique (Stamnes et al., 1991). This method is based on the comparison between two ratios of irradiances at two selected wavelengths (one where the ozone absorption is strong and the other where it is weak). One ratio is simulated beforehand and is stored in a look up table (LUT) and the other is calculated from the UV measurements (Houët and Brogniez, 2004). The ozone absorption cross-sections used to calculate the LUT are taken from Paur and Bass at 221 K (1985). With this technique, it is possible to retrieve ozone under clear sky and cloudy conditions. A previous study (Brogniez et al., 2005) has shown that under cloudy conditions the daily ozone mean is a rather good estimation of the true value. The uncertainties on the ozone retrieval are about 3% on clear sky and about 7% on cloudy days. So, in this study daily averages of the ground-based data obtained for all sky conditions and for zenith angles smaller than 75° are compared with OMI values obtained during overpass.

### 2.1.2 UV irradiance

Erythemal dose rate are computed from ground-based spectra using CIE action spectrum (Diffey and McKinlay, 1987) and erythemal daily dose are computed integrating the erythemal dose rate over the day.

To carry out comparison of two spectra measured by two instruments with slit functions of different FWHM one has to process the spectra to set them at a common FWHM (Slaper et al., 1995; Bais et al., 2001). Therefore, the ground-based spectra were first deconvoluted using their own FWHM and then reconvoluted with a triangular slit function with FWHM of 0.55 nm in order to make the spectroradiometer irradiance comparable to the spectral irradiances produced by the OMI surface UV algorithm. The processing was carried out using the SHICrivm tool (Slaper et al., 1995).

## 2.2 Ozone Monitoring Instrument

OMI is a Dutch/Finnish instrument onboard the NASA Earth Observing System (EOS) Aura spacecraft (Levelt et al., 2006a). OMI is a nadir-viewing UV/Visible spectrometer with a spectral resolution about 0.63 nm for the visible channel (349–504 nm) and about 0.42 nm for the UV channel (307–383 nm). It measures the solar light scattered by the atmosphere in the 270–500 nm wavelength range with a spatial resolution at nadir of 13 km×24 km. The sun-synchronous orbit of Aura and the wide viewing angle of OMI enable daily global coverage of the sunlit portion of the Earth. OMI is the successor of the Total Ozone Mapping Spectrometer (TOMS) instruments and contributes to monitoring of the atmospheric ozone, trace gases, aerosols and surface UV radiation (Levelt et al., 2006b).

### 2.2.1 OMI total column ozone data

Two algorithms are used to derive the total column of ozone from OMI measurements. One of the two algorithms is the TOMS Version 8 algorithm (Bhartia et al., 2002). The





same algorithm was used to reprocess all the TOMS data since 1978. It uses two wavelengths to derive total ozone, 317.5 and 331.2 nm under most conditions, 331.2 and 360 nm for high ozone and high solar zenith angle and also other wavelengths for quality control.

The relative uncertainty on this OMI-TOMS-like product is around 2% for solar zenith angle lower than 70° and increasing to 5% at 85° according to Bhartia et al. (2002).

The other algorithm developed at KNMI (the Netherlands) is based on the Differential Optical Absorption Spectroscopy (DOAS) technique. In the DOAS algorithm, the TOC is determined in three steps. In the first step, to obtain the so-called slant column density (the amount of ozone along an average photon path from the Sun to the satellite), the actual DOAS fitting is performed. In the second step, the air mass factor is determined, which is needed to convert the slant column density into a vertical column. The third step consists of a correction for cloud effects. According to Veefkind et al. (2006), the relative uncertainty on this OMI-DOAS-like product is about 3% for cloudy days and 2% for clear days.

### 2.2.2 OMI surface UV data

The algorithm used to estimate the UV radiation reaching the Earth's surface is similar to the algorithm used to retrieve UV from the TOMS data (Herman et al., 1999; Krotkov et al., 2002). This OMI surface UV algorithm is based on the use of a radiative transfer model using the OMI-derived total ozone and cloud information as input parameters for modelling. The surface albedo data are obtained from a climatology based on the Nimbus-7/TOMS measurements (Tanskanen, 2004). First of all, the clear-sky surface irradiance is calculated and then a correction is made taking into account the attenuation of the UV radiation by clouds and scattering aerosols (Tanskanen et al., 2006). The speed of the algorithm is optimized using precalculated lookup tables. The OMI surface UV algorithm produces estimates of erythemal daily dose as well as local solar noon erythemal irradiance and spectral irradiances at 305.1, 310.1, 324.1 and 380.1 nm which are calculated using a triangular slit function whose FWHM is 0.55 nm.

For validation purposes a modified version of the OMI surface UV algorithm was used to produce for VdA a time series of OMI-derived erythemal dose rate and spectral irradiances corresponding to the OMI overpass time. In the future these additional products will be added to the standard OMUVB product.

The accuracy of the OMI-derived daily doses was assessed in a recent validation study (Tanskanen et al., 2007). According to the validation results the OMI-derived daily erythemal doses have a median overestimation of 0–10% for flat, snow-free regions with modest loadings of absorbing aerosols or trace gases, and some 60 to 80% of the doses are within ±20% from the ground reference. For sites significantly affected by absorbing aerosols or trace gases the positive bias can be up to 50%. Because the aerosol absorption cross sections tend to increase as the wavelength decreases, even bigger biases are expected for the low wavelength spectral irradiances derived from the OMI measurements. Thus, comparison of the OMI-derived spectral irradiances with the ground-based measurements will contribute to understanding of the effect of aerosols on surface UV as well as further development of the OMI surface UV algorithm.

## 3 Results

### 3.1 Ozone comparisons

We present scatter plots of the TOC derived from the ground-based instrument at both sites and from OMI derived with the two techniques and also time series of the relative differences (OMI-GB)/GB in percent, where GB represents the TOC from the ground-based instrument.

Figure 1a shows the comparison between the TOC retrieved in Briançon and the TOC OMI-TOMS-like, for the period October 2004–September 2005 considering all sky conditions.

(The comparison with the TOC OMI-DOAS-like is not presented for Briançon since





the data are not available for the previous period.)

Figure 1b presents the time series of the relative difference, with cloudy sky data plotted as cross, clear sky data as black points and with the snow-covered surface data as blue squares.

Accounting for the uncertainties on both products, the comparison is rather satisfying but we note a negative bias (TOC spectroradiometer > TOC OMI) about −3.1 % (Table 1), with discrepancies more important in summer. This seasonal effect can be explained by a cloud effect since clear sky data (black dots) show no seasonal variation. In this study, the days with snow-covered ground (blue squares) show no particular effect. If we consider only the clear days, the comparison is slightly better, the equation of the regression line is $y=0.99x-7.1$ with a correlation coefficient equal to 0.99.

When looking at relative differences versus the solar zenith angle (SZA) corresponding to OMI data (Fig. 1c), the largest discrepancies observed in summer (smallest SZA) are confirmed for cloudy sky condition data. For clear sky the dependency is small.

Figures 2a–c present the results for the site of VdA for OMI-TOMS-like method for the period October 2005–February 2007.

The scatter plot in Fig. 2a shows similar results as in Fig. 1a.

In Fig. 2b no obvious seasonal effect appears for cloudy days (cross) but in case of clear sky (black dots), the seasonal effect appears unambiguously, OMI TOC is smaller than GB TOC in summer while it is generally the reverse (or no difference) during the rest of the year. If we look at Fig. 2c, we notice that, for the majority of points with large SZA for all sky conditions, OMI TOC is greater than GB TOC.

For the comparison on clear sky days, the relative differences do not exceed 5%, the correlation coefficient is 0.98 and the equation of the regression line is $y=0.98x+7.6$ much satisfying that for all sky conditions.

Figures 2d–f present the results for the site of VdA for OMI-DOAS-like method for the same period as previously.

Considering the Figs. 2e and f, obviously there is a seasonal effect for both clear and cloudy sky condition data. Dependence with SZA is very important even by clear sky.





The regression line for only clear sky data is $y=0.99x+6.3$ much better than for all sky conditions with a correlation coefficient equal to 0.96. The agreement is better particularly in summer, with relative differences lower than 5%.

To summarize, in VdA we have a better agreement between the ground-based TOC and OMI-TOMS-like TOC (RMS=3.2% and the average of relative difference equal 0.5%, Table 1) than with the other method (RMS=4.7%, the average of the relative difference equal 1.9%, Table 1) and there is a strong SZA effect.

### 3.2 Surface UV comparisons

#### 3.2.1 Spectral UV

OMI spectral irradiances are available in VdA at the time of overpass. Figure 3a shows the comparison with the spectroradiometer at wavelength 324.1 nm and Fig. 3b shows the comparison at wavelength 380.1 nm for the period October 2005–December 2006 only for clear sky conditions. The correlations are excellent at both wavelengths but we observe that there is a bias at 324.1 nm and that the regression line is worse at 380.1 nm.

The relative difference is plotted versus the spectral irradiance measured by the spectroradiometer in Fig. 3c (324.1 nm) and in Fig. 3d (380.1 nm). The bias observed in Fig. 3a appears clearly; moreover we can note larger differences for low irradiance (Figs. 3c–d).

If we look at the plot of the relative difference versus SZA (Fig. 3e), we see larger discrepancies for SZA>65° at both wavelengths with OMI>GB in most cases. For these SZA, the irradiance is low and the uncertainty on the measurements with the ground-based spectroradiometer is larger than at smaller SZA. Only one measurement obtained for SZA=53° gives differences larger than the average values at both wavelengths (violet cross and circle).

Under clear sky conditions, the aerosol optical thickness (AOT) is routinely retrieved from the spectroradiometer measurements (Brogniez et al., 2008), the lower wave-

length at which AOT is retrieved with confidence is 330 nm. Figures 3f and g show that there exists a weak correlation between the differences and the AOT for most days, larger relative differences correspond to larger AOT. But larger differences at larger SZA (Fig. 3e) are not systematically explained by large aerosol contents (the AOT for these days are small). Concerning the point for 324.1 nm (violet cross) at SZA equal to 53° (Fig. 3e), the larger AOT (0.47) seems to be the reason of the relative difference equal to 23% (Fig. 3f). Similarly for the wavelength 380.1 nm (violet cross in Fig. 3g), the AOT equal to 0.47 explains the relative difference equal to 15%.

### 3.2.2 Erythemal dose rate

OMI-derived erythemal dose rates (EDR) are also available for VdA at the time of overpass. Figure 4a shows the comparison with the spectroradiometer and Fig. 4b shows the comparison with the broadband radiometer for the period October 2005–February 2007 for all sky conditions. In both cases, the OMI surface UV algorithm overestimates the dose rate.

The relative differences (OMI-GB)/GB studied versus the cloud optical depth at 360 nm (COD) that is derived by the OMI surface UV algorithm, show a dependence (Fig. 4c). The difference between OMI and GB is more important for large COD. A similar study of the relative difference versus the distance between the OMI pixel and the VdA site shows no correlation (not shown).

The same comparison conducted on spectroradiometer data for clear skies only (Fig. 4d) exhibits the same behaviour, however the number of pairs is small (54 points). The points are less scattered than for all sky conditions, (the correlation coefficient is equal to 0.99).

As can be seen in Fig. 4e, a weak correlation exists between the relative difference and the aerosol content. The bias appears bigger at bigger values of AOT and for small erythemal dose rate (Fig. 4f).

### 3.2.3 Erythemal daily dose

Figure 5a shows the scatter plot of the erythemal daily dose (EDD) derived from OMI and from the spectroradiometer in Briançon for the period October 2004–September 2005 for all sky conditions.

Time series of the relative differences are shown in Fig. 5b. The data pairs are grouped in three classes: clear-sky, cloudy sky, and snow-covered surface (cloudy or not).

It appears that when the ground is covered with snow, the OMI-derived daily dose is generally lower than the ground-based measurement, with large relative difference. The surface albedo used by the OMI surface UV algorithm is a climatological one, and likely it was lower than the actual effective surface albedo at least during the validation campaign.

If we consider all the data, the average of relative difference is 8% but when excluding snowy days, there is a positive bias for the majority of points (generally in summer) and the average of relative difference is about 14% (Table 2).

Figure 5c compares the erythemal daily dose in VdA for the period October 2005–July 2006 for all sky conditions.

In VdA, a positive bias appears (OMI>GB) also as Briançon excluding snowy days, the average of relative difference is about 17% for all sky conditions (Table 2). For clear sky days (black dots), the relative differences are smaller, they do not exceed 22%, but the bias remains (Fig. 5d), the average of relative difference is about 13%.

As was mentioned in Sect. 2.2.2, the bias is observed in a previous validation work conducted with measurements at several sites (Tanskanen et al., 2007).

## 4 Summary

The previous results from the scatter plots are summarized in Table 1 for ozone, in Table 2 for UV. For each comparison, we report the number of data pairs





and in parentheses the number of points ($n$), the correlation coefficient ($r$), the slope and the intercept of the regression line, the RMS $\left(=\sqrt{\frac{1}{n}\sum_{i=1}^{n}(y_i - x_i)^2}\right)$, the %RMS $\left(=\sqrt{\frac{1}{n}\sum_{i=1}^{n}\left(\frac{y_i - x_i}{x_i}\right)^2}\times 100\right)$ and the mean relative difference in % $\left(=\frac{1}{n}\sum_{i=1}^{n}\left(\frac{y_i - x_i}{x_i}\right)\times 100\right)$.

## 5 Conclusion

The aim of this study was to validate OMI products with measurements performed by ground-based UV instruments located at two French sites. A spectroradiometer and a broadband radiometer were operating at VdA and there was a spectroradiometer at Briançon.

The comparison of the total column of ozone shows a satisfying agreement at both sites for the OMI-TOMS-like product. For the OMI-DOAS-like product, the comparison conducted at VdA is less satisfying that with OMI-TOMS-like product and a seasonal variation of the agreement appears. This phenomenon is related to a SZA effect and has been reduced in the new version of the data (collection 3, overpass files not yet available).

For this validation campaign a modified version of the OMI surface UV algorithm was used to provide irradiances at 324.1 and 380.1 nm and OMI erythemal dose rates at the time of overpass at VdA.

Spectral UV comparisons are satisfying except at low irradiance level (large SZA). Comparisons of OMI erythemal dose rates show an overestimation of the ground-based dose rates. The same effect appears for the erythemal daily doses. For the site of Briançon, for most days OMI overestimates also ground-based erythemal daily doses, whereas when the ground is covered with snow, it is the opposite. These ob-

served biases between OMI erythemal dose rates, OMI erythemal daily doses and ground-based data are in agreement with previous results obtained at other sites, including snow-covered surface cases (Tanskanen et al., 2007).

The study of the impact of the AOT on the quality of the agreement show that large AOT values can explain few large discrepancies between ground-based and satellite UV products.

The better agreement observed for spectral UV compared to the erythemal daily dose and dose rate can be explained considering that the erythemal doses concern a shorter wavelength range and that the validation of spectral irradiance at 305 and 310 nm is not included in the current validation work.

*Acknowledgements.* We thank C. Deroo and F. Ducos for their efficient help in handling data. We thank also T. Cabot and A. de la Casinière for taking care of the Briançon instrument. The sites are supported by CNES within the french program TOSCA.

The figures were drawn using the Mgraph package developed at LOA by L. Gonzalez and C. Deroo (http://www-loa.univ-lille1.fr/Mgraph/)

The Dutch-Finnish built OMI instrument is part of the NASA EOS Aura satellite payload. The OMI project is managed by NIVR and KNMI in the Netherlands. We thank the OMI International Science Team for the satellite data used in this study. The OMI surface UV data were obtained from the NASA Aura Validation Data Center (AVDC). This work was performed in the framework of the International ESA/KNMI/NIVR OMI "Announcement of Opportunity for Calibration and Validation of the Ozone Monitoring Instrument", providing early access to provisional OMI data sets and guidance to public OMI data.

OMI overpass data is available through the Aura Validation Data Center (AVDC, http://avdc.gsfc.nasa.gov).

## References

Bais, A., Gardiner, B., Slaper, H., et al.: SUSPEN intercomparison of ultraviolet spectroradiometers, J. Geophys. Res., 106(D12), 12 509–12 525, 2001.





Bhartia, P. K. and Wellemeyer, C.: TOMS-V8 Total O3 Algorithm, in: OMI ATBD, Volume II, OMI ozone product, edited by: Bhartia, P. K., 2002.

Bernhard, G. and Seckmeyer, G.: Uncertainty of measurements of spectral solar UV irradiance, J. Geophys. Res., 104, 14 321–14 345, 1999.

Brogniez, C., Houët, M., Siani, A. M., Weihs, P., Allaart, M., Lenoble, J., Cabot, T., de La Casinière, A., and Kyro, E.: Ozone column retrieval from solar UV measurements at ground level: Effects of clouds and results from six European sites, J. Geophys. Res., 110, D24202, doi:10.1029/2005JD005992, 2005.

Brogniez, C., Buchard, V., and Auriol, F.: Validation of UV-visible aerosol optical thickness retrieved from spectroradiometer measurements, Atmos. Chem. Phys. Discuss., 8, 3895–3919, 2008, http://www.atmos-chem-phys-discuss.net/8/3895/2008/.

Herman, J. R., Krotkov, N., Celarier, E., Larko, D., and Labow, G.: Distribution of UV radiation at the Earth's surface from TOMS-measured UV-backscattered radiances, J. Geophys. Res., 104, 12 059–12 076, 1999.

Houët, M.: Spectroradiométrie du rayonnement Solaire UV au sol: Améliorations apportées à l'instrumentation et au traitement des measures, Analyse pour l'évaluation du contenu atmosphérique en ozone et en aérosols, Ph.D. thesis, Univ of Lille, France, 2003.

Houët, M. and Brogniez, C.: Ozone column retrieval from solar UV irradiance measurements at ground level: sensitivity tests and uncertainty estimation, J. Geophys. Res., 109, D15302, doi:10.1029/2004JD004703, 2004.

Krotkov, N. A., Herman, J., Bhartia, P. K., Seftor, C., Arola, A., Kaurola, J., Kalliskota, S., Taalas, P., and Geogdzhaev, I.: Version 2 TOMS UV algorithm: problems and enhancements, Opt. Eng., 41, 3028–3039, 2002.

Levelt, P. F., van den Oord, G. H. J., Dobber, M. R., Mälkki, A., Visser, H., de Vries,, J., Stammes, P., Lundell, J. O. V., and Saari, H.: The Ozone Monitoring Instrument, IEEE Trans. Geosc. Remote Sens., 44(5), 1093–1101, 2006a.

Levelt, P. F., Hilsenrath, E., Leppelmeier, G. W., van den Oord, G. B. J., Bhartia, P. K., and Tamminen, J.: Science Objectives of the Ozone Monitoring Instrument, IEEE Trans. Geosc. Remote Sens., 44(5), 1199–1208, 2006b.

Paur, R. J. and Bass, A. M.: The ultraviolet cross sections of ozone. II, Results and temperature dependence, in: Atmospheric Ozone, Proceedings of the Quadriennal Ozone Symposium, edited by: Zerefos, C. and Ghazi, A., 611–616, 1985.





Slaper, H., Reinen, H., Blumthaler, M., Huber, M., and Kuik, F.: Comparing ground-level spectrally resolved solar UV measurements using various instruments: a technique resolving effects of wavelength shift and slit width, Geophys. Res. Lett., 22(20), 2721–2724, 1995.

Stamnes, K., Slusser, J. R., and Bowen, M.: Derivation of total ozone abundance and cloud effects from spectral irradiance measurements, Appl. Opt., 30, 4418–4426, 1991.

Tanskanen, A.: Lambertian surface albedo climatology at 360 nm from TOMS data using moving time-window technique, in: Proceedings of the 20th Quadriennal Ozone Symposium, Kos, Greece, 1159–1160, 2004.

Tanskanen, A., Lindfors, A., Määttä, A., Krotkov, N., Herman, J., Kaurola, J., Koskela, T., Lakkala, K., Fioletov, V., Bernhard, G., McKenzie, R., Kondo, Y., O'Neill, M., Slaper, H., den Outer, P., Bais, A., and Tamminen, J.: Validation of daily erythemal doses from Ozone Monitoring Instrument with ground-based UV measurement data, J. Geophys. Res., 112, D24S44, doi:10.1029/2007JD008830, 2007.

Tanskanen, A., Krotkov, N. A., Herman, J. R., and Arola, A.: Surface Ultraviolet Irradiance from OMI, IEEE Trans. Geosc. Remote Sens., 44, 5, 1267–1271, 2006.

Veefkind, J. P., de Haan, J. F., Brinksma, E. J., Kroon, M., and Levelt, P. F.: Total Ozone from the Ozone Monitoring Instrument (OMI) using the DOAS technique, IEEE Trans. Geosc. Remote Sens., 44, 5, 1239–1244, 2006.

WMO: Scientific Assessment of Ozone depletion: 2006, WMO Report no. 50, 2007.





**Table 1.** Summary of TOC OMI validation results.

| | *n* | *r* | slope | intercept | RMS | Mean relative difference |
|---|---|---|---|---|---|---|
| Briançon TOC (OMI TOMS-like) | 348 | 0.98 | 0.95 | 6.1 | 13.8 DU (4.1%) | −3.1% |
| clear sky Briançon TOC (OMI TOMS-like) | 78 | 0.99 | 0.99 | −7.1 | 11.9 DU (3.7%) | −3.2% |
| VdA TOC (OMI TOMS-like) | 662 | 0.97 | 0.96 | 15.1 | 10.4 DU (3.2%) | 0.5% |
| clear sky VdA TOC (OMI TOMS-like) | 56 | 0.98 | 0.98 | 6.7 | 6.2 DU (1.9%) | 0.1% |
| VdA TOC (OMI DOAS-like) | 684 | 0.95 | 0.95 | 22.1 | 15 DU (4.7%) | 1.9% |
| clear sky VdA TOC (OMI DOAS-like) | 56 | 0.96 | 0.99 | 4.9 | 10.6 DU (3.3%) | 1.4% |



ACPD
8, 4309–4351, 2008



**Table 2.** Summary of UV OMI validation results.

| | *n* | *r* | slope | intercept | RMS | Mean relative difference |
|---|---|---|---|---|---|---|
| VdA EDR OMI=f(spectroradiometer) | 723 | 0.96 | 1.08 | 4.4 | 16.5 mW/m$^2$ (58%) | 32.5% |
| clear sky VdA EDR OMI=f(spectroradiometer) | 54 | 0.99 | 1.14 | 0.5 | 14.7 mW/m$^2$ (20%) | 16.8% |
| VdA EDR OMI=f(radiometer) | 627 | 0.96 | 1.13 | 6.2 | 17.1 mW/m$^2$ (110%) | 69.3% |
| clear sky VdA EDR OMI=f(radiometer) | 45 | 0.99 | 1.14 | 4.2 | 15.1 mW/m$^2$ (45%) | 38.9% |
| Briançon EDD OMI=f(spectroradiometer) | 293 | 0.97 | 1.22 | −154 | 514 J/m$^2$ (24%) | 7.9% |
| clear sky Briançon EDD OMI=f(spectroradiometer) | 64 | 0.98 | 1.3 | −224 | 613 J/m$^2$ (19%) | 7.3% |
| VdA EDD OMI=f(spectroradiometer) | 349 | 0.99 | 1.14 | 16.6 | 340 J/m$^2$ (27.5%) | 17.1% |
| clear sky VdA EDD OMI=f(spectroradiometer) | 33 | 0.99 | 1.13 | 2.3 | 340 J/m$^2$ (13.5%) | 13% |
| clear sky VdA Spectral UV 324.1 nm | 49 | 0.99 | 1.0 | 8.3 | 12.5 mW/m$^2$/nm (8.8%) | 6.4% |
| clear sky VdA Spectral UV 380.1 nm | 49 | 0.99 | 0.95 | 25 | 21.5 mW/m$^2$/nm (8.4%) | 3.7% |



ACPD
8, 4309–4351, 2008



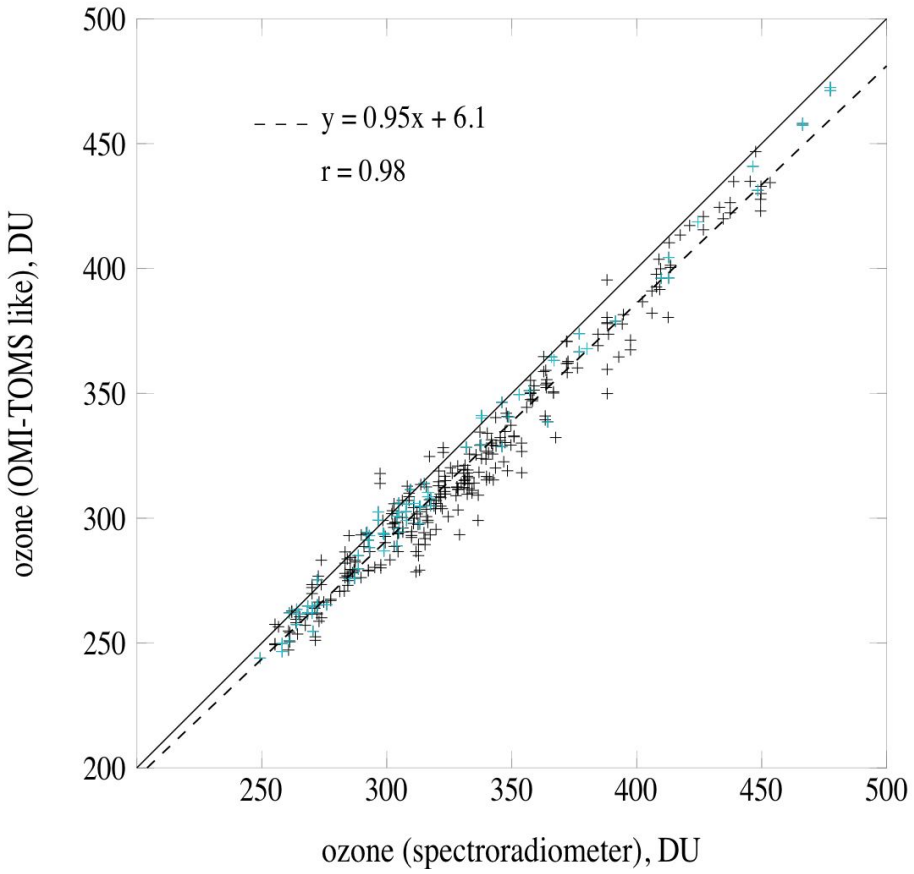


**Fig. 1. (a)** Comparison between TOC from the ground-based instrument in Briançon and from OMI-TOMS-like method for all sky conditions (blue cross represents snowy surface days). The equation of the regression line (dash line) and the correlation coefficient are indicated, the solid line is the first bisector.

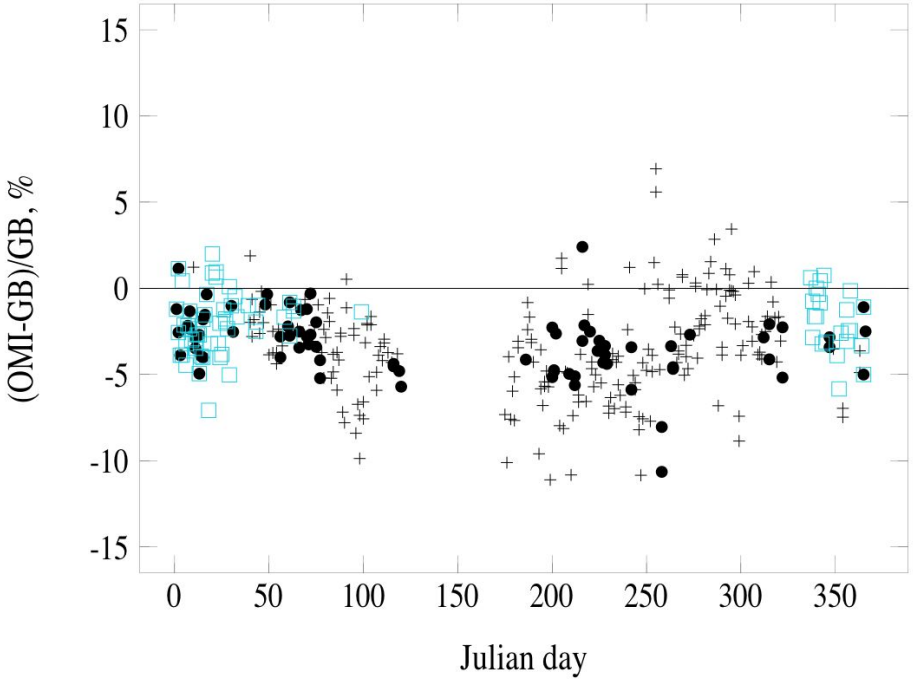


**Fig. 1. (b)** Time series of the relative differences between ground-based and OMI-TOMS-like TOC in Briançon (cross represent cloudy day data, black dots represent clear days and blue squares represent snowy surface days, black dots inside a blue squares for clear snowy days).



ACPD
8, 4309–4351, 2008



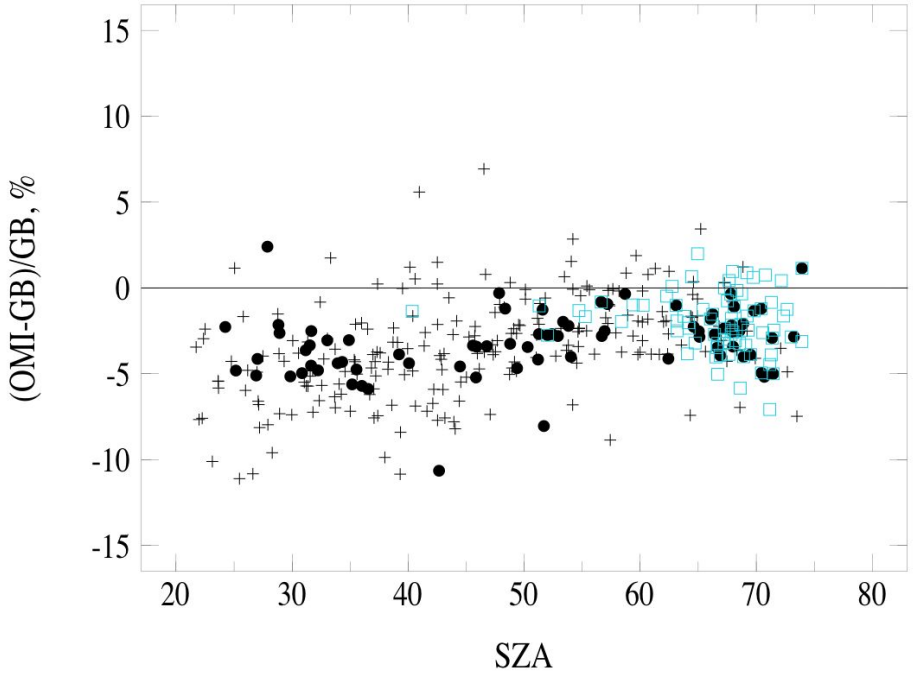


**Fig. 1. (c)** Relative difference between ground-based and OMI-TOMS-like TOC in Briançon versus SZA (cross represent cloudy day data, black dots represent clear sky days and blue squares represent snowy surface days, black dots inside a blue squares for clear snowy days).



ACPD
8, 4309–4351, 2008



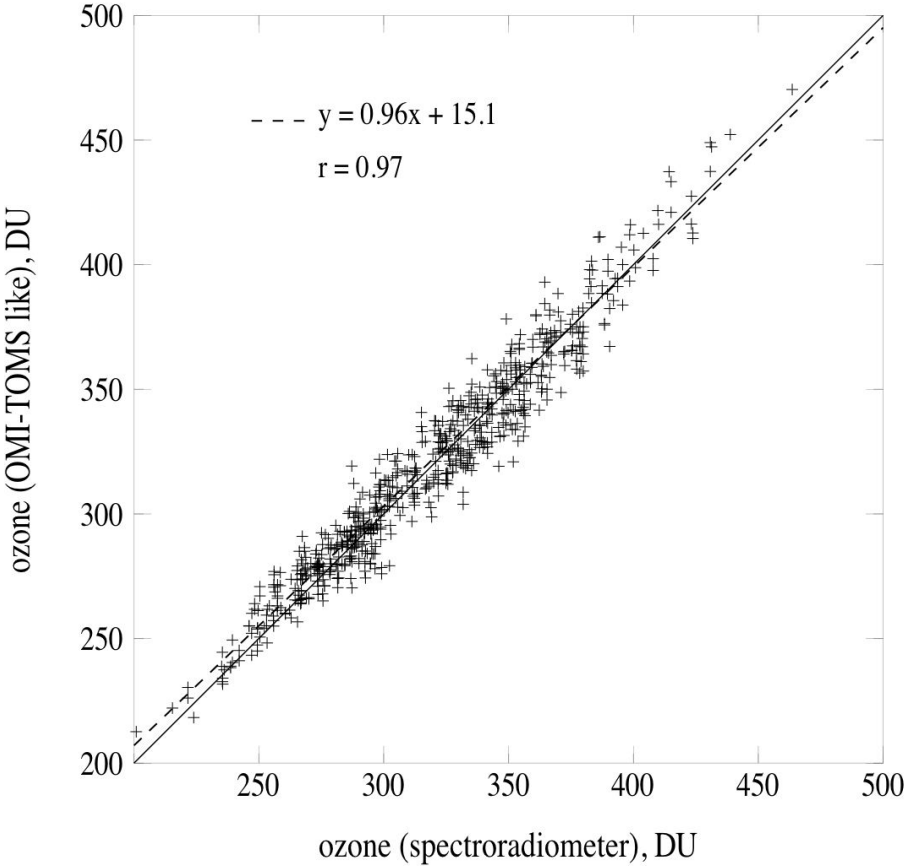


**Fig. 2. (a)** Same as Fig. 1a for OMI-TOMS-like method but in VdA.



ACPD
8, 4309–4351, 2008

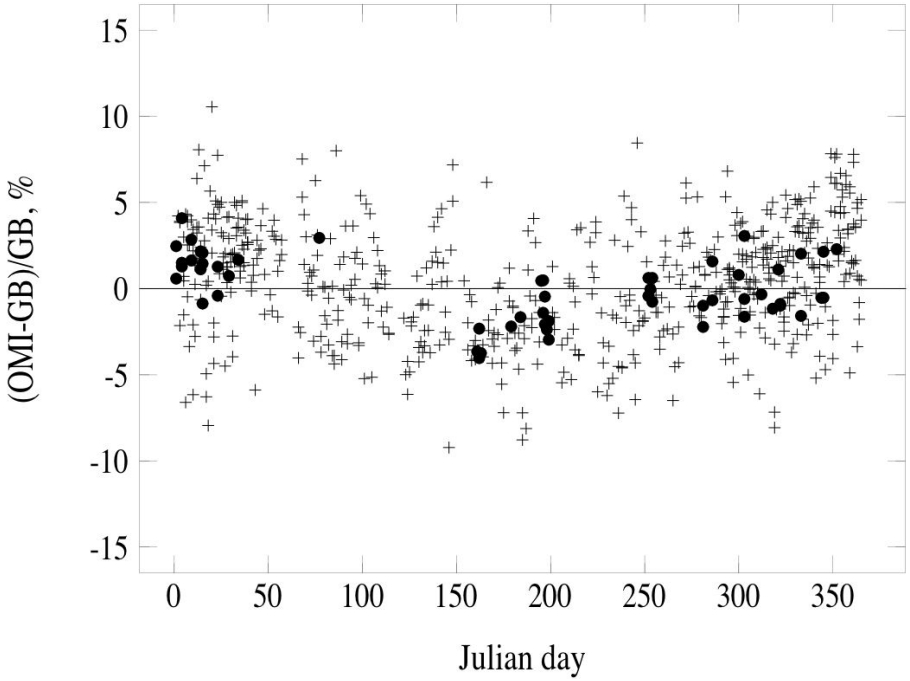


**Fig. 2. (b)** Same as Fig. 1b for OMI-TOMS-like method but in VdA.



ACPD
8, 4309–4351, 2008



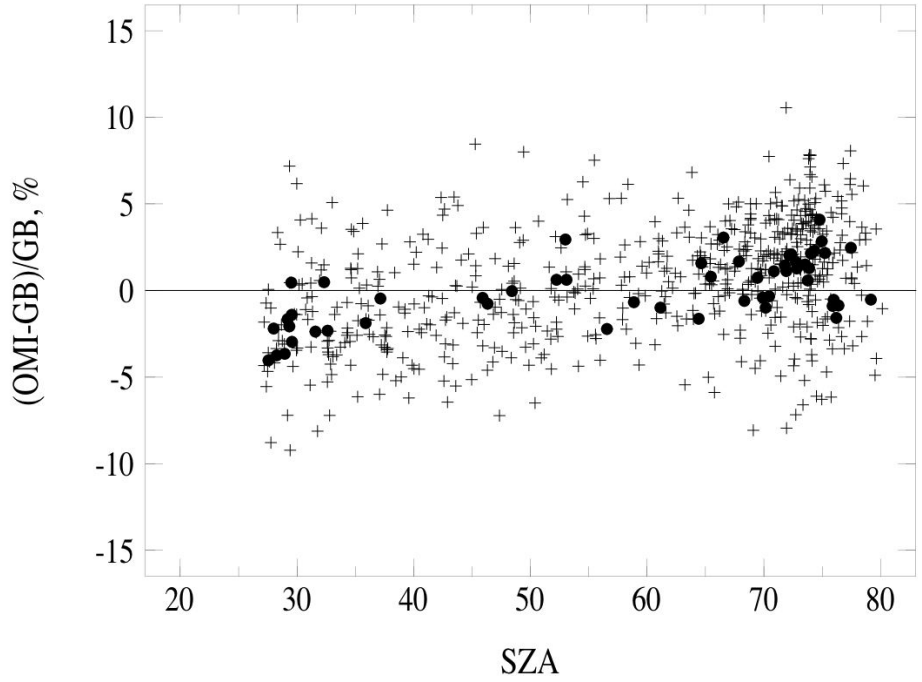


**Fig. 2. (c)** Same as Fig. 1c for OMI-TOMS-like method but in VdA.



ACPD
8, 4309–4351, 2008



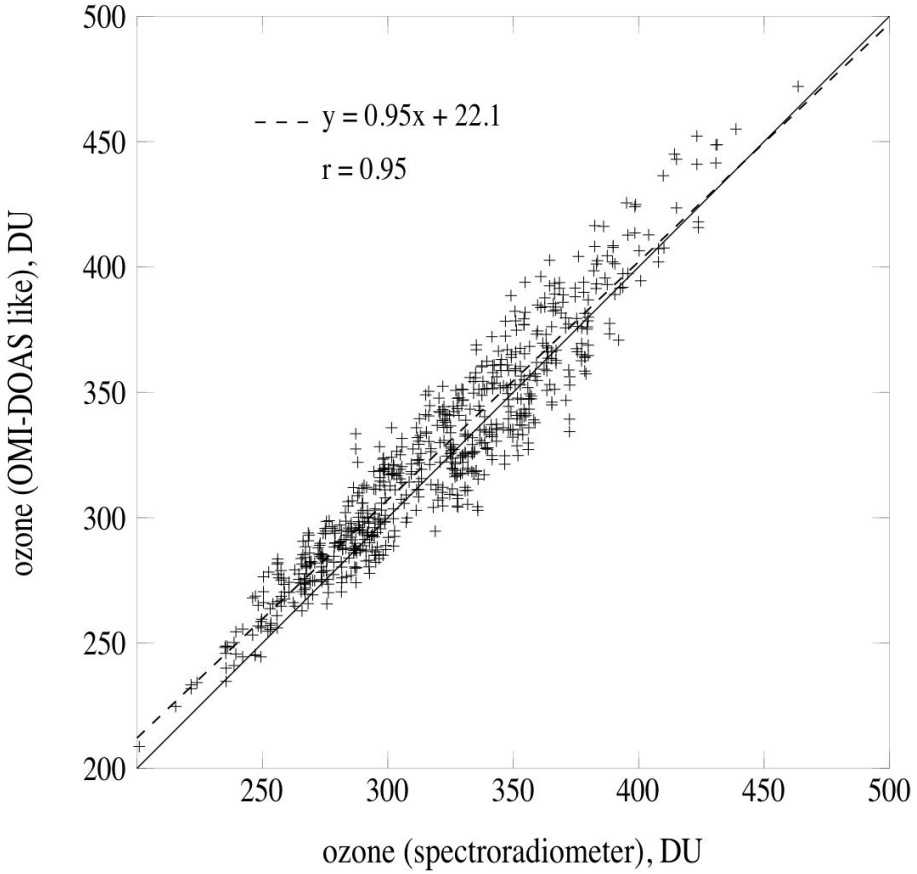


**Fig. 2. (d)** Same as Fig. 2a but for TOC from OMI-DOAS-like method.



ACPD
8, 4309–4351, 2008



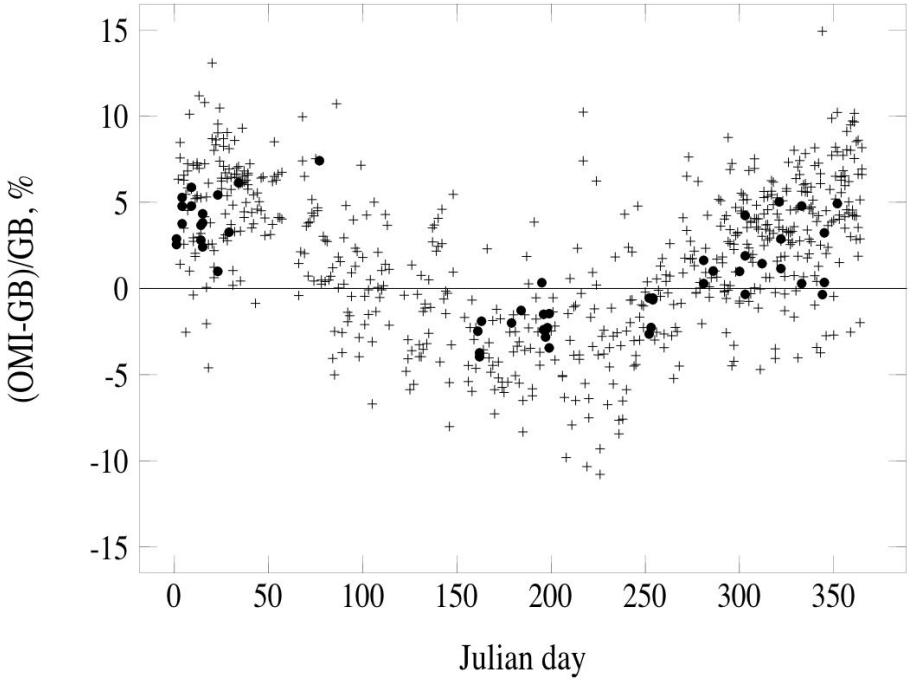


**Fig. 2. (e)** Same as Fig. 2b but for TOC from OMI-DOAS-like method.



ACPD
8, 4309–4351, 2008



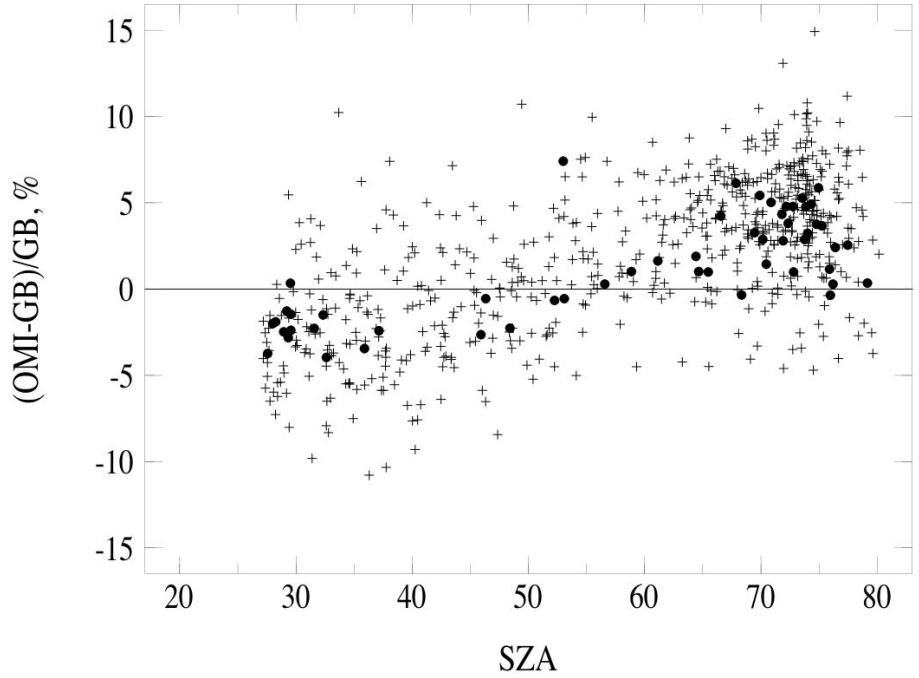


**Fig. 2. (f)** Same as Fig. 2c but for TOC from OMI-DOAS-like method.

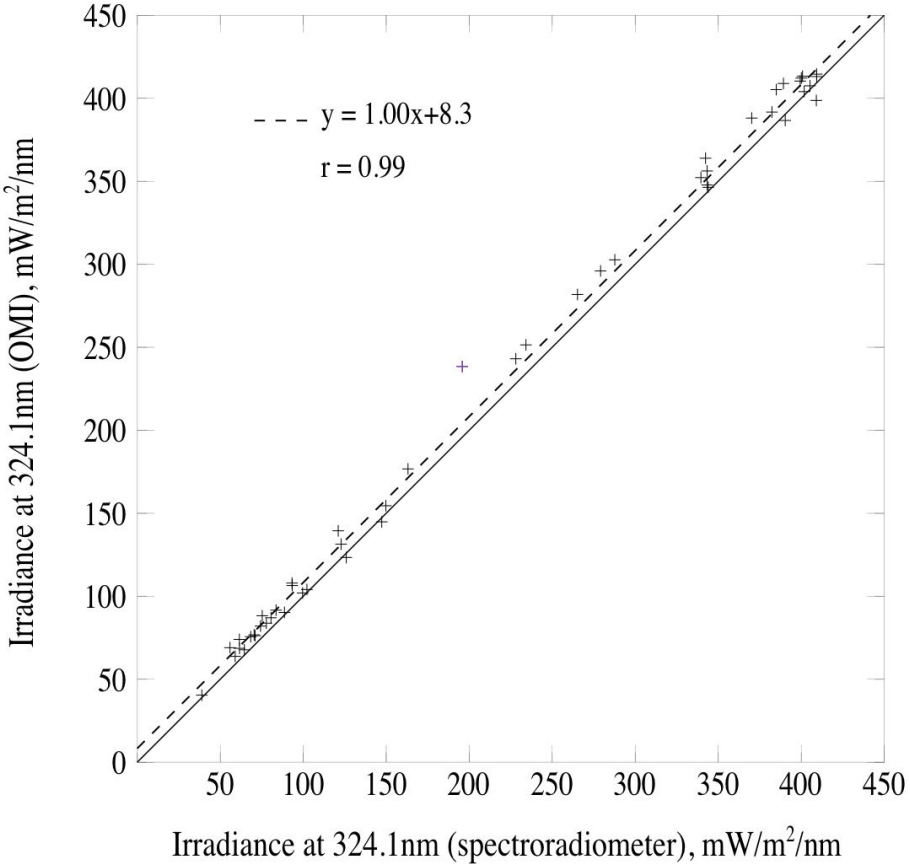


**Fig. 3. (a)** Comparison between spectral irradiance at 324.1 nm from the spectroradiometer in VdA and from OMI at the time of overpass for clear skies (the violet cross is studied later).



ACPD
8, 4309–4351, 2008



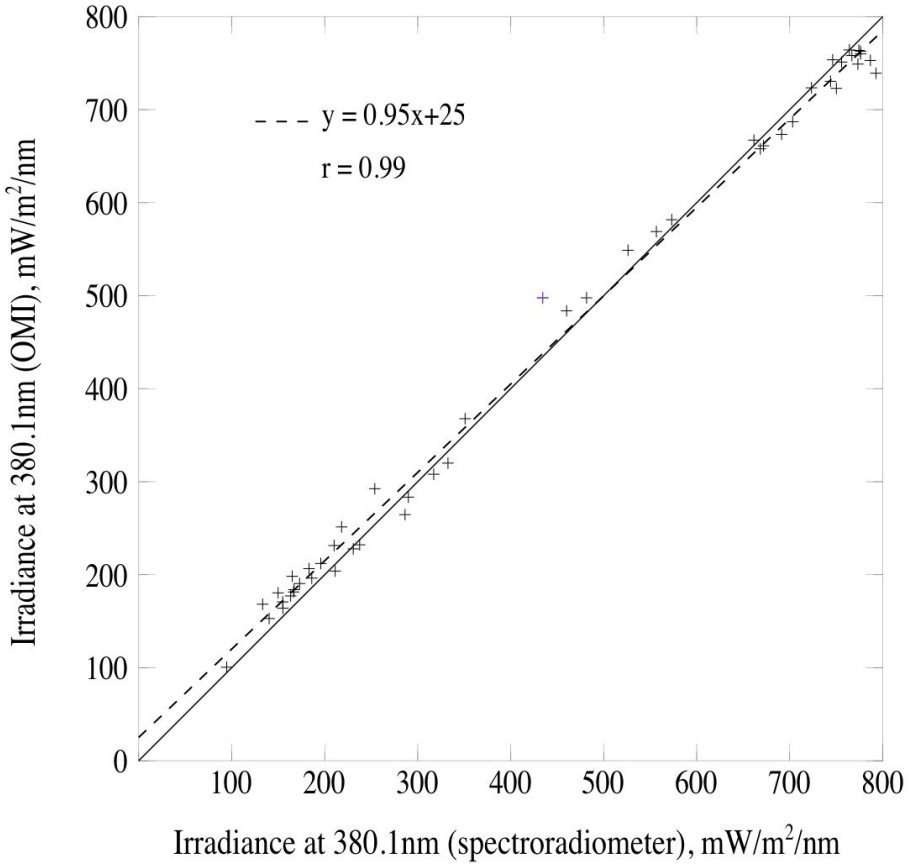


**Fig. 3. (b)** Same as Fig. 3a but at 380.1 nm.

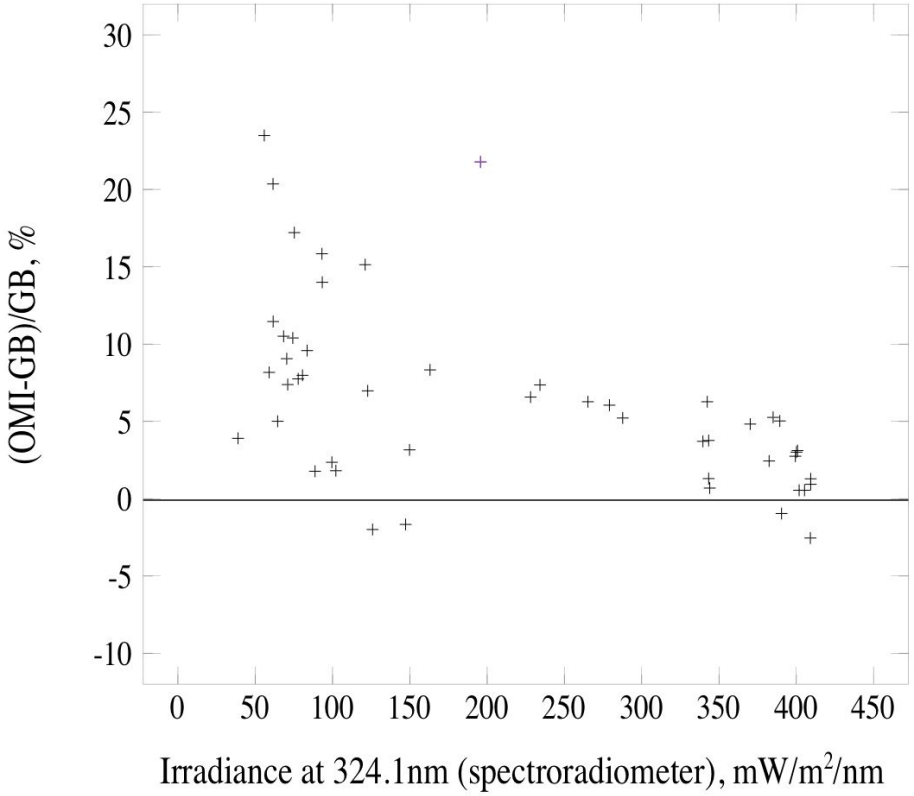


**Fig. 3. (c)** Relative differences between ground-based and OMI spectral irradiance at 324.1 nm as a function of the spectroradiometer irradiance in VdA for clear skies.

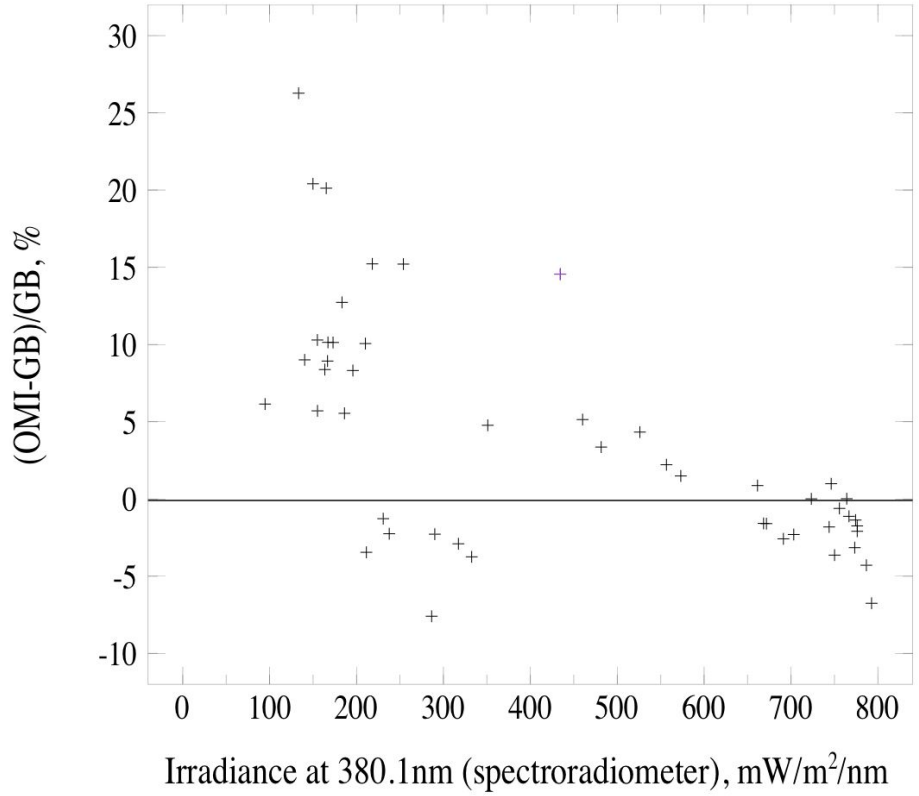


**Fig. 3. (d)** Same as Fig. 3c for 380.1 nm.

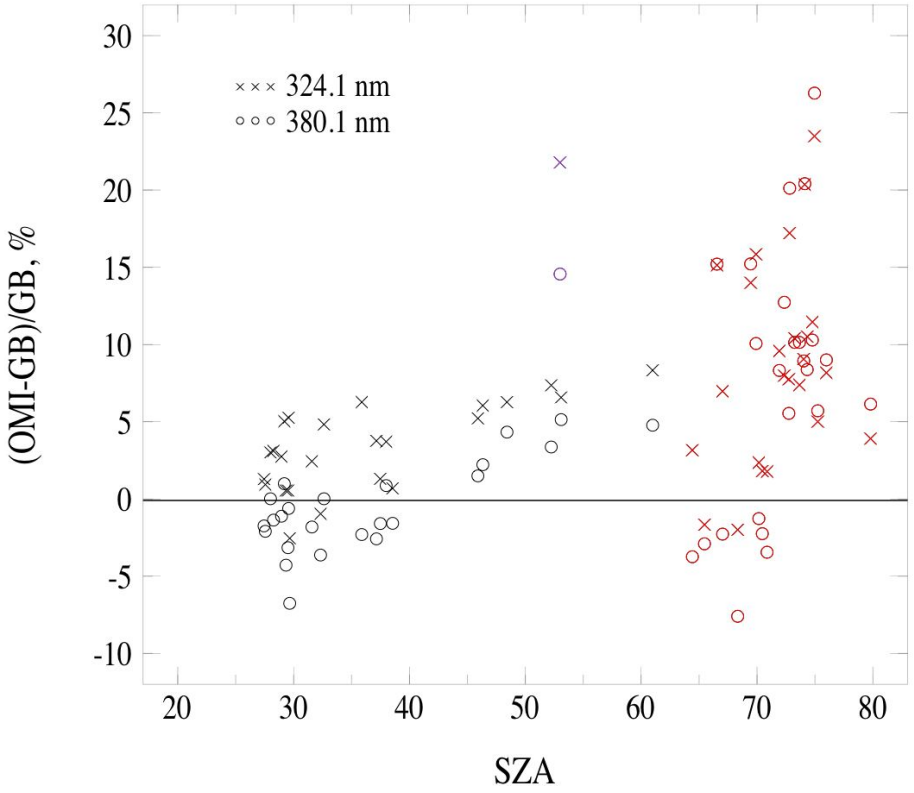


**Fig. 3. (e)** Relative differences between ground-based and OMI spectral irradiance for both wavelengths as a function of SZA in VdA for clear skies. (red cross and circle for SZA>65°).



ACPD
8, 4309–4351, 2008



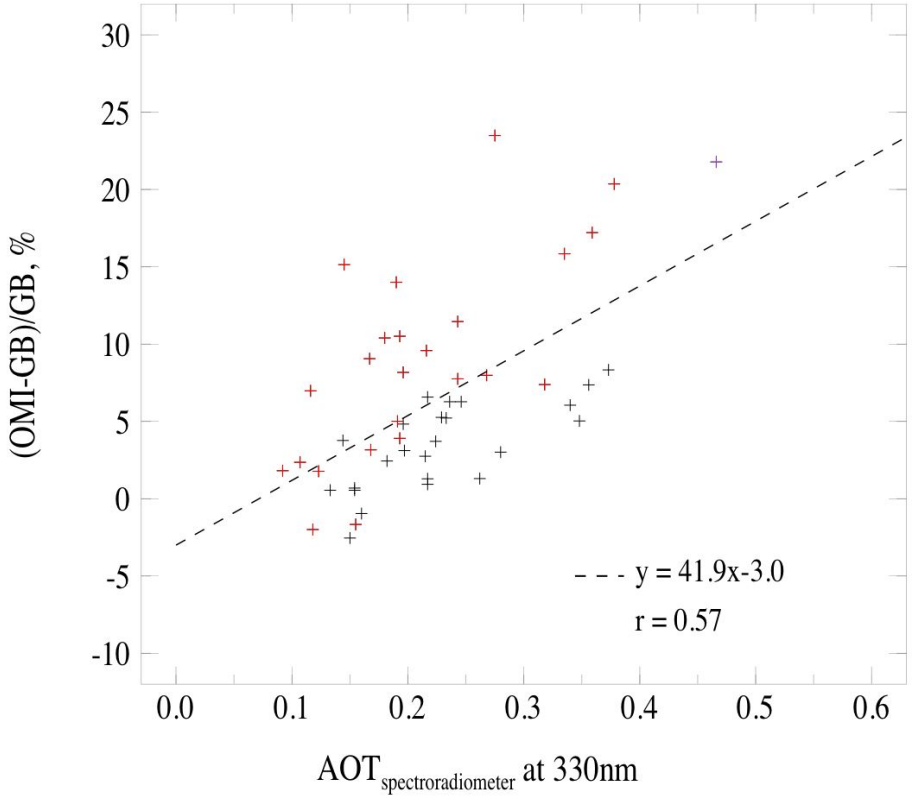


**Fig. 3. (f)** Relative differences between ground-based and OMI spectral irradiance at 324.1 nm as a function of AOT at 330 nm in VdA for clear skies (red cross for SZA>65°).



ACPD
8, 4309–4351, 2008

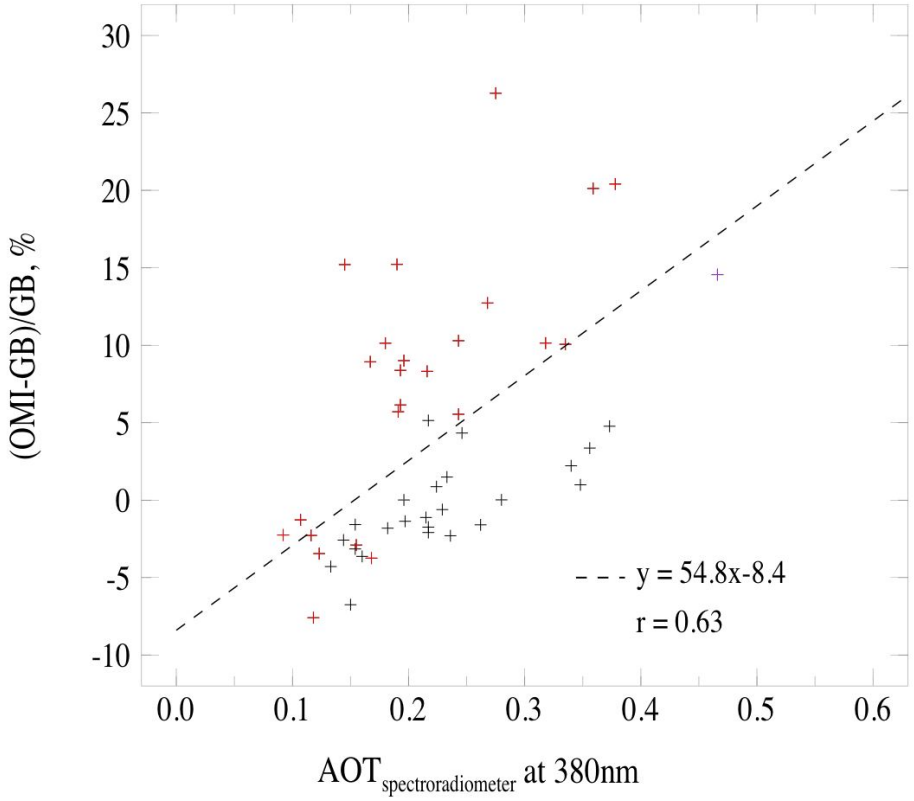


**Fig. 3. (g)** Relative differences between ground-based and OMI spectral irradiance at 380.1 nm as a function of AOT at 380 nm in VdA for clear skies (red cross for SZA>65°).

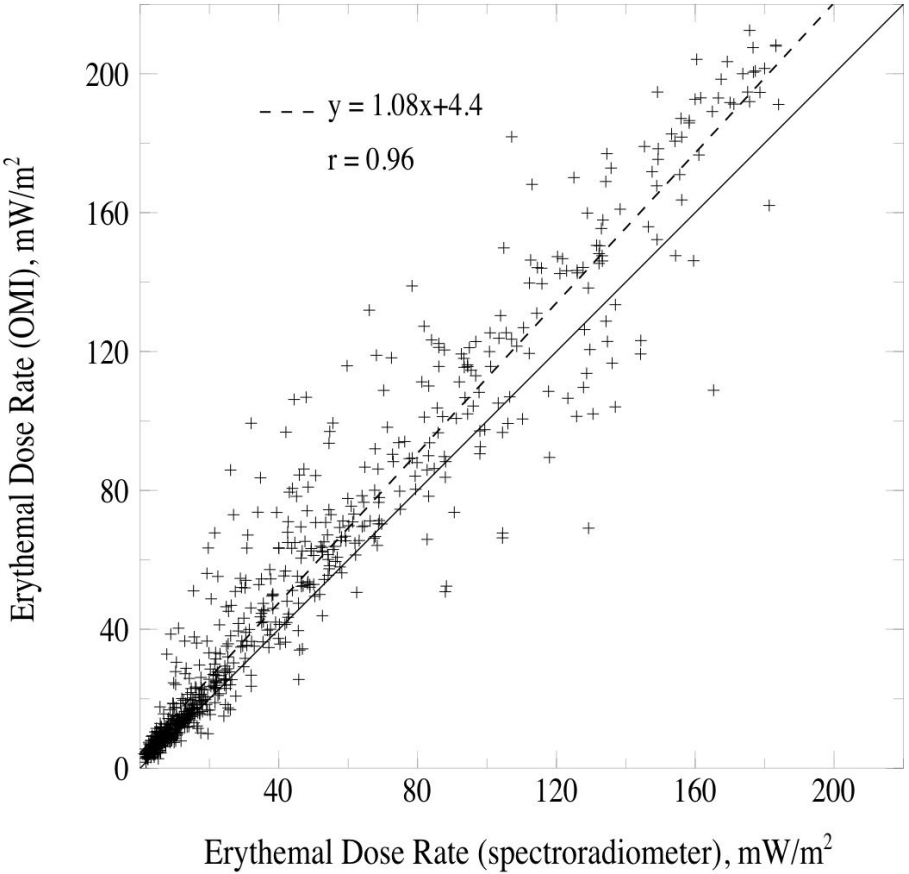


**Fig. 4. (a)** Comparison between erythemal dose rate from the spectroradiometer in VdA and erythemal dose rate from OMI at the time of overpass. The equation of the regression line (dash line) and the correlation coefficient are indicated, the solid line is the first bisector.



ACPD
8, 4309–4351, 2008

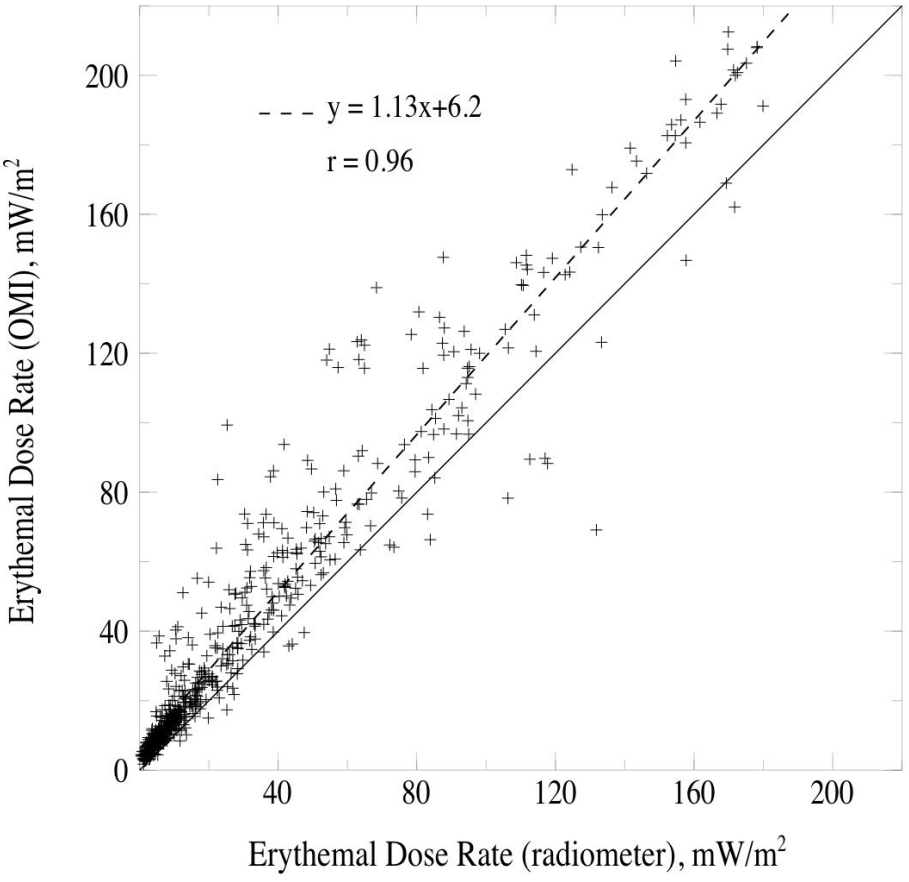


**Fig. 4. (b)** Same as Fig. 4a but for the broadband radiometer.



ACPD
8, 4309–4351, 2008



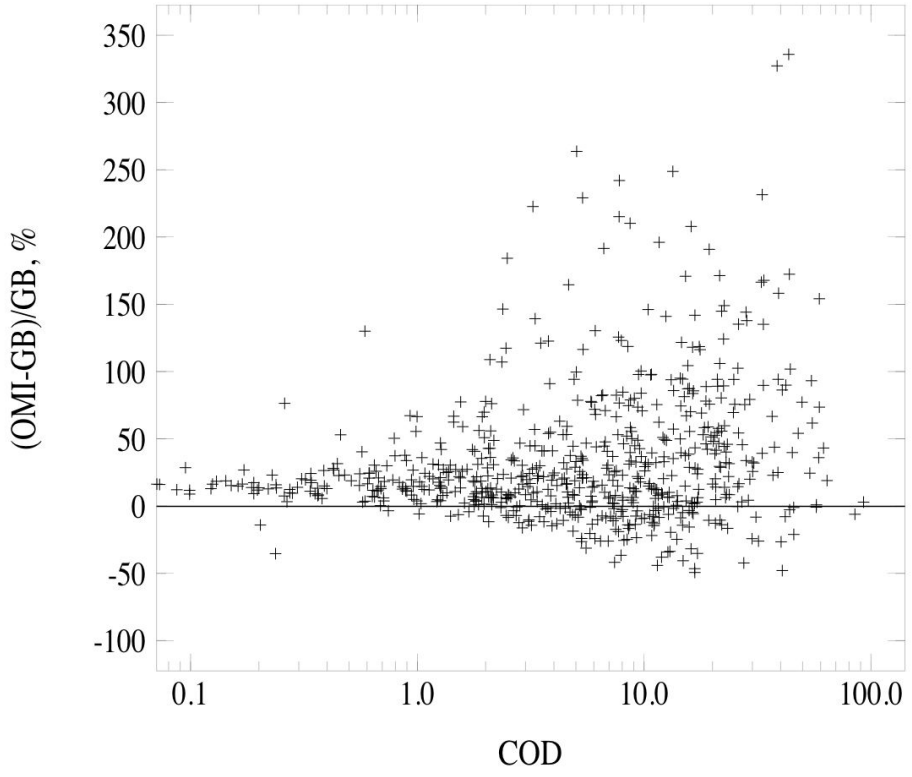


**Fig. 4. (c)** Relative difference of erythemal dose rates (OMI-spectro)/spectro as a function of COD in VdA for all sky conditions.



ACPD
8, 4309–4351, 2008



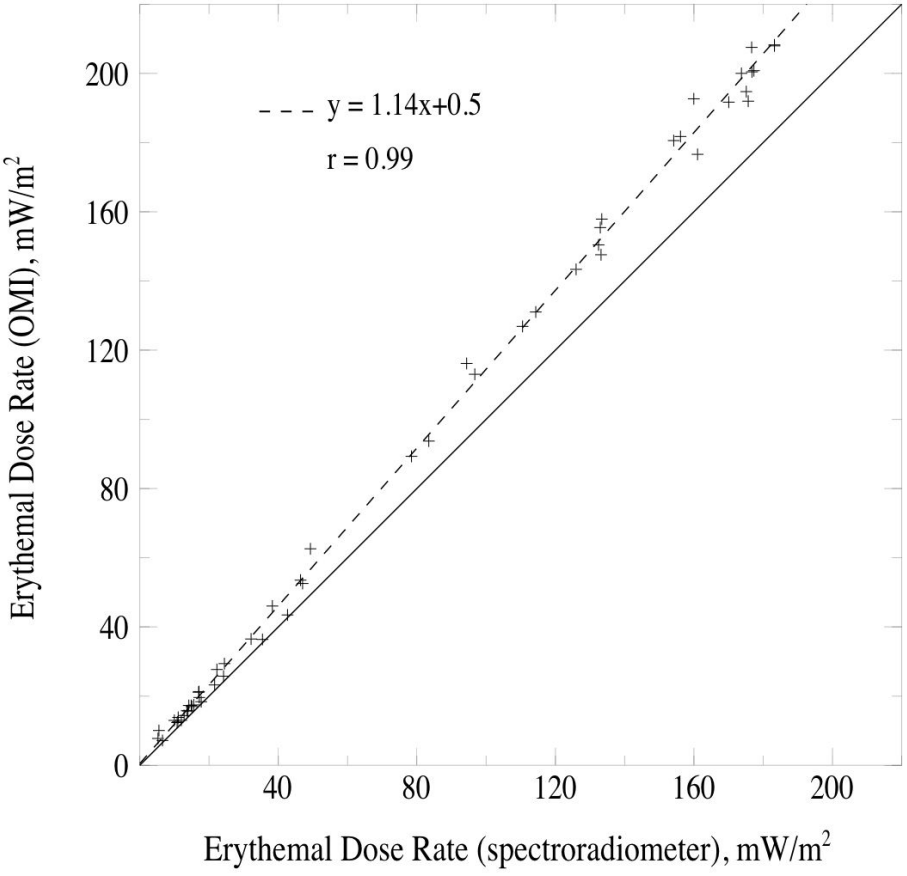


**Fig. 4. (d)** Same as Fig. 3a but for clear skies only.



ACPD
8, 4309–4351, 2008

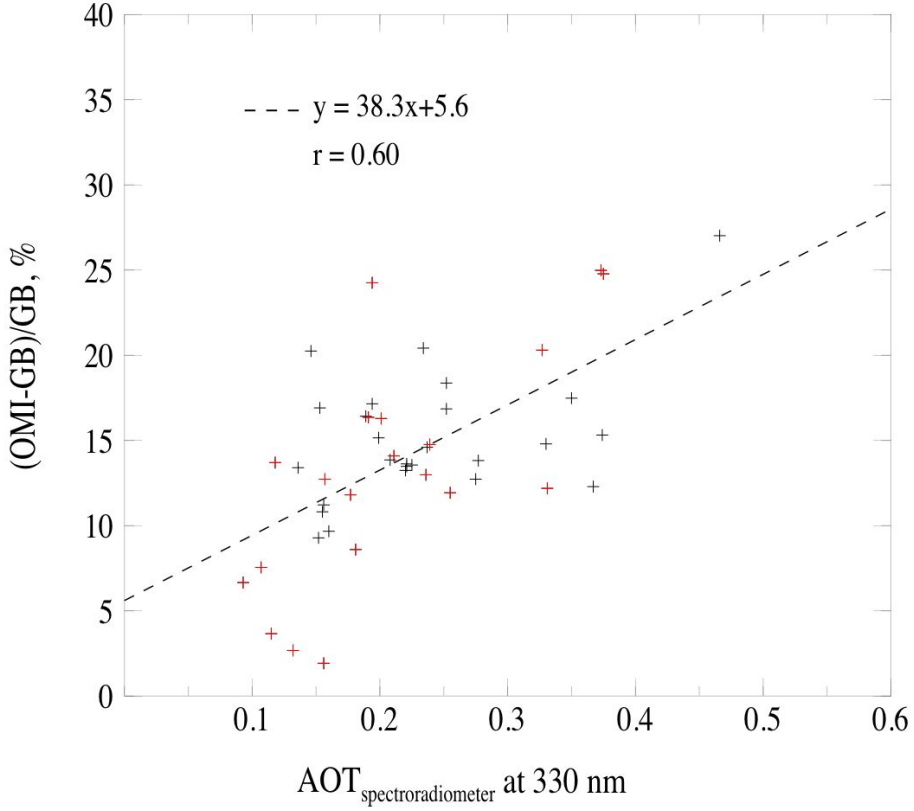


**Fig. 4. (e)** Relative difference of erythemal dose rates (OMI-spectro)/spectro as a function of AOT at 330 nm in VdA for clear skies (red cross for SZA>65°).

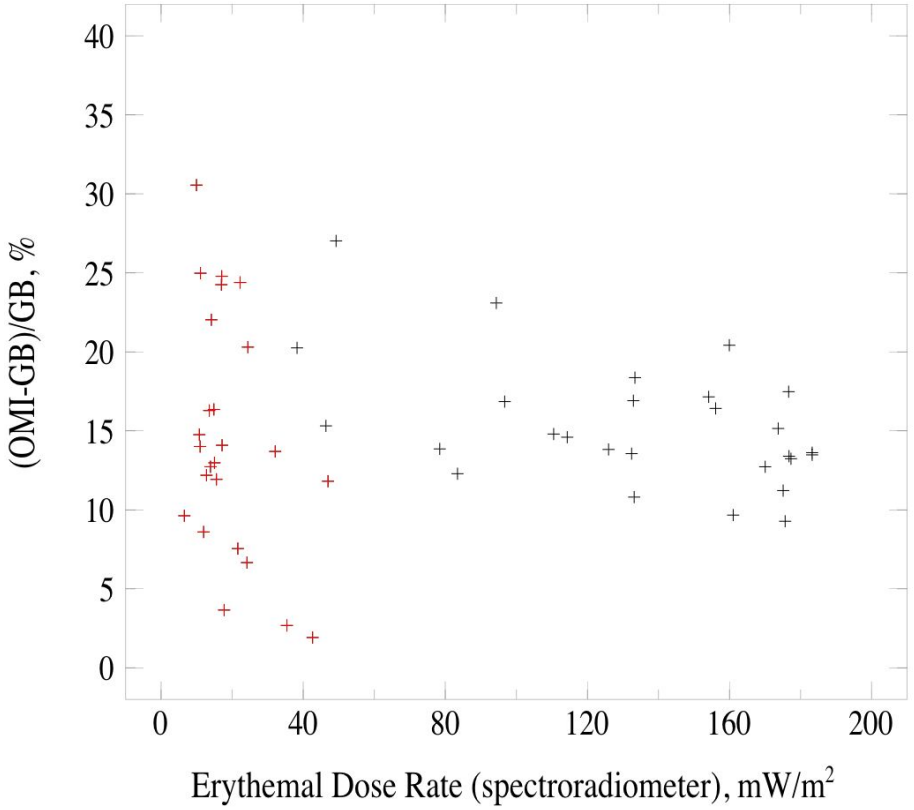


**Fig. 4. (f)** Relative difference of erythemal dose rates (OMI-spectro)/spectro as a function of the spectroradiometer erythemal dose rate in VdA for clear skies (red cross for SZA>65°).

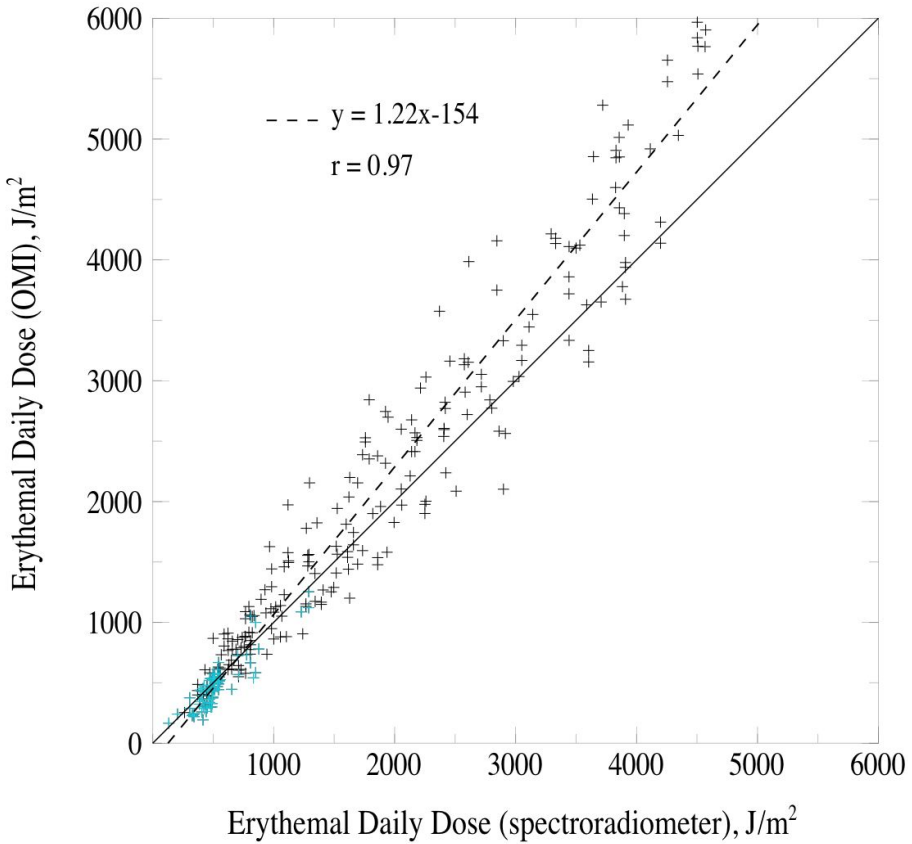


**Fig. 5. (a)** Comparison between erythemal daily doses from the spectroradiometer in Briançon and from OMI. The blue cross indicate snowy surface. The equation of the regression line (dash line) and the correlation coefficient are indicated, the solid line is the first bisector.



ACPD
8, 4309–4351, 2008

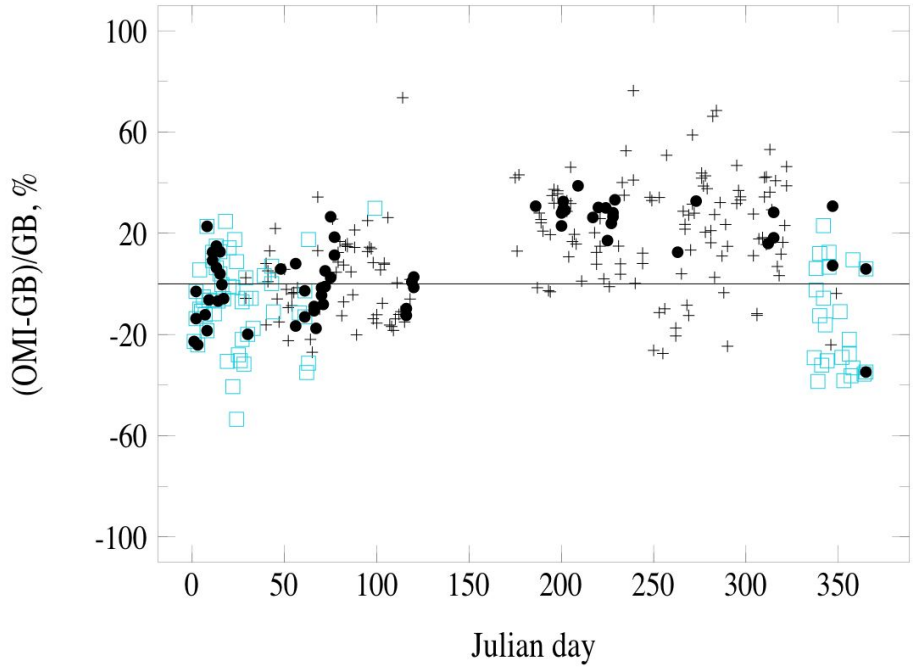


**Fig. 5. (b)** Time series of the relative differences between ground-based and OMI erythemal daily dose in Briançon (cross for cloudy day, blue squares are for snowy surface and black dots are for clear days, black dots inside a blue squares for clear snowy days).

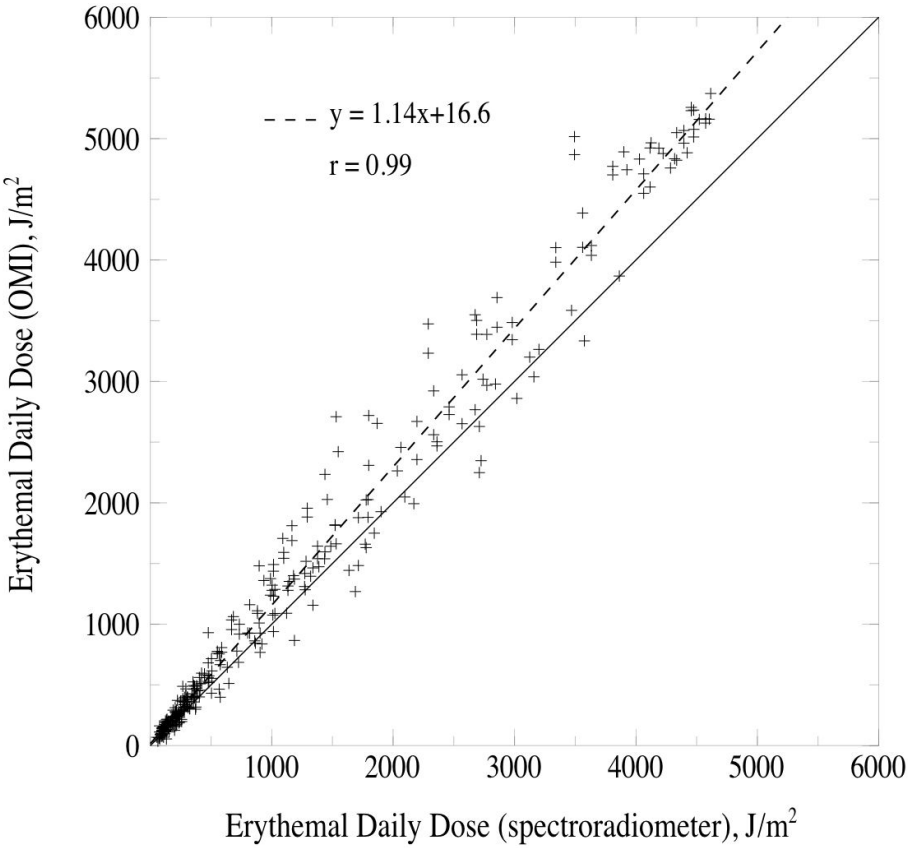


**Fig. 5. (c)** Same as Fig. 5a but in VdA.

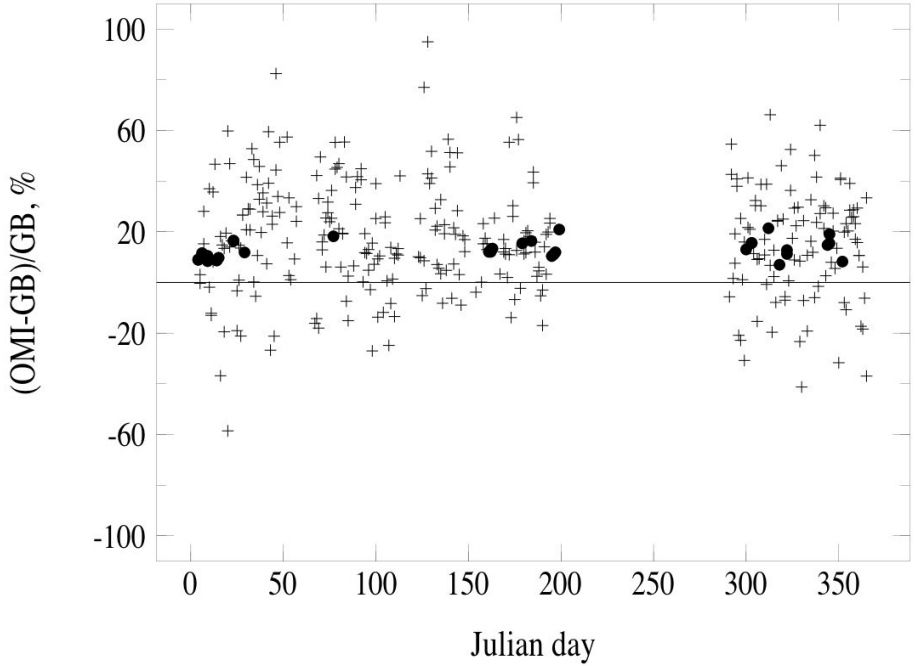


**Fig. 5. (d)** Same as Fig. 5b but in VdA.



ACPD
8, 4309–4351, 2008